An Interactive Barnes Objective Map Analysis Scheme for Use with Satellite and Conventional Data

STEVEN E. KOCH

Goddard Laboratory for Atmospheric Sciences, NASA Goddard Space Flight Center, Greenbelt, MD 20771

MARY DESJARDINS

Information Extraction Division, NASA/Goddard Space Flight Center, Greenbelt, MD 20771

PAUL J. KOCIN

Goddard Laboratory for Atmospheric Sciences, NASA/Goddard Space Flight Center, Greenbelt, MD 20771

(Manuscript received 11 December 1982, in final form 1 June 1983)

ABSTRACT

An objective analysis scheme based on the Barnes technique and designed for use on an interactive computer is described. In order to meet the specific needs of the research meteorologist, the interactive Barnes scheme allows real-time assessments both of the quality of the resulting analyses and of the impact of satellite-derived data upon various meteorological data sets. Display of a number of statistical and mapped analysis quality control indicators aid the impact assessments. Simple means for taking account of the spatially clustered nature typical of satellite data are included in the internal computations of the relative weights of data at grid point locations.

An analyst is allowed the capability of modifying values of certain input parameters to the interactive Barnes scheme within internally set limits. These constraints were objectively determined and tested in a number of different situations prior to implementation. The following constraints are employed: 1) calculation of the weights as a function of a data spacing representative of the data distribution; 2) automatic elimination of detail at wavelengths smaller than twice the representative data spacing; 3) placement of bounds upon the grid spacing by the data spacing; and 4) setting of a fixed limit on the number of passes through the data to achieve rapid and sufficient convergence of the analyzed values to the observed ones. A mathematical analysis of the convergence properties of the Barnes technique is presented to support the validity of the latter constraint.

Despite these constraints, the interactive Barnes scheme remains versatile because it accepts limited inputs to the data and grid display areas, to the data and grid spacings, and to the rate of convergence of the analysis to the observations. Input parameter values are entered through a series of questions displayed on a computer video terminal and by manipulation of display function devices. The analyst immediately sees a plot of the data, the contoured grid values, superimposed in various colors if desired, and the effects of choice of analysis options. Examples of both meteorological and satellite data analyses are presented to demonstrate the objectivity, versatility and practicality of the interactive Barnes scheme.

1. Introduction

For several years, meteorological satellites have provided high quality fields of atmospheric temperature, moisture, and winds. Yet, their potential for enhancing mesoscale analyses and forecasts cannot be realized until certain problems in interpretation and assimilation are solved. In the case of satellite cloud motion wind data, high quality data sets are now available for mesoscale analysis (Hasler *et al.*, 1977; Wilson and Houghton, 1979; Peslen, 1980; Negri and Vonder Haar, 1980). However, the problems of assigning accurate cloud heights and placing the data onto a coordinate surface which minimizes errors due to vertical wind shear must be solved prior to their insertion into numerical prediction models (Peslen *et al.*, 1982). Also, the smallest scale at which new information can be provided by satellite-derived data has yet to be determined.

Moisture and temperature profiles retrieved from multispectral infrared and microwave sensors aboard polar-orbiting satellites (Smith, *et al.*, 1979) have been available for several years for weather analysis (Hayden, 1973; Horn, *et al.*, 1976) and large-scale numerical weather prediction (Tracton, *et al.*, 1980). A major advance in the area of remotely determined soundings occurred recently when the Visible and Infrared Spin-Scan Radiometer (VISSR) Atmospheric Sounder (VAS) was added to the Geostationary Operational Environmental Satellites (GOES).

The VAS instrument produces data from up to 12 infrared channels in addition to the visible, and makes possible frequent soundings of temperature and moisture needed for mesoscale analysis (Chesters *et al.*, 1982). Initial results indicate VAS can depict meaningful patterns of mid-level dryness, low level moisture, and mesoscale regions of potential instability (Petersen *et al.*, 1982). Yet, these data can be used quantitatively only after their useful spatial resolution and compatibility with conventional rawinsonde data have been objectively determined.

The cloud motion wind and VAS data types are both highly non-uniformly distributed in space. Satellite winds are characteristically available in clusters because trackable clouds exist in clumps, whereas satellite soundings can be retrieved only where substantial cloud cover is *not* present. The analysis of either satellite data alone or of satellite data combined with meteorological data must take into account the spatial clustering problem before the issues of spatial resolution and compatibility can be addressed.

An assessment needs to be made of the impact that merger of high quality, high resolution data from these remote sensors with conventional data has upon the analysis and prediction of mesoscale processes relevant to severe convective storm development and evolution. At the NASA Goddard Laboratory for Atmospheric Sciences (GLAS), experience has shown that satellite impact assessments can be more readily made when the capability exists to analyze objectively the data sets composed of data from different observing systems (satellite, conventional, special network, etc.), with the analysis results made available in real time. This capability has been achieved with an interactive software program which has as its foundation the Barnes (1973) objective analysis technique. The interactive Barnes scheme has been developed with the multiple aims of 1) obtaining analyses resulting from use of objective constraints, 2) having a scheme that is versatile enough to account for the particular characteristics of combined data sets, and 3) implementing the scheme on an interactive computer so that it is both practical and fast. The scheme is implemented on an interactive, minicomputer-based processing and display system known as the Atmospheric and Oceanic Image Processing System (AOIPS), described in detail by Billingsley (1976) and Heymsfield *et al.* (1983). Other real-time data analysis and display systems include the MCIDAS at the University of Wisconsin (Smith, 1975), the ADVISAR at Colorado State University (Smith *et al.*, 1978), the Pennsylvania State analysis and forecasting system (Cahir *et al.*, 1981), and the workstation developed by PROFS (Reynolds, 1983).

The interactive Barnes scheme is an integral part of a softward package on AOIPS known as GEMPAK (General Meteorological data assimilation, analysis, and display software Package). GEMPAK enables the research meteorologist to create discrete files of data, to analyze numerous fields, to merge different types of data file structures and to display the analyses. The user interacts with GEMPAK through terminal commands and function control switches on AOIPS. Manipulation of these various devices allows the user to quickly alter and visualize changes in the contoured analyses that result from changes in the values of the input parameters to the scheme. Furthermore, analyses of different meteorological variables or different data sets can be overlaid by combining images from several memory channels in different colors.

The interactive Barnes scheme is designed with features that attempt to account for the highly non-uniform distribution of satellite data and which also tackle the problems of merging satellite and conventional data. Negri and Vonder Haar (1980), Peslen (1980) and others show that computed kinematic fields are highly sensitive to the clustered nature of trackable clouds in satellite imagery. Other problems lie in the interpretation of an objective analysis near boundaries and in knowing how much smoothing is justified. Objective constraints are built within this scheme to deal with all these problems.

The next section discusses the characteristics of the Barnes (1973) objective map analysis scheme that make it particularly adaptable to these needs. Section 3 shows how the scheme is specifically tailored to meet those needs. Section 4 is concerned with the effects of input parameter variations upon objective analyses of various kinds of data sets. These analyses have been made to assess the impact 1) of satellite-derived winds upon SESAME (Severe Environmental Storms and Mesoscale Experiment) rawinsonde wind data (Peslen, *et al.*, 1982), 2) of VAS soundings upon synoptic-scale rawinsonde data and upon the ability to delineate potential regions of severe convective development (Petersen *et al.*, 1982), and 3) of SESAME regional and storm-scale rawinsonde data upon the ability to diagnose frontal and jet streak-related processes at the subsynoptic scale (Uccellini and Kocin, 1981). The Appendix contains a proof of numerical convergence for the Barnes (1973) scheme and a demonstration that two passes through the data provide sufficient convergence of the analyzed values to the observed ones. A detailed explanation of the stepwise procedure that is taken in conducting a GEMPAK Barnes objective map analysis can be found in Koch *et al.* (1981).

2. Characteristics of the Barnes objective map analysis scheme suitable for implementation on an interactive computer

The Barnes (1973) objective map analysis scheme is a computationally simple, Gaussian weighted-averaging technique which assigns a weight to a datum solely as a known function of distance between datum and grid point. The weight w_m is assigned according

to the distance r_m between the datum $f(x_m, y_m)$ and the (i, j) grid point as

$$w_m = \exp\left(-\frac{r_m^2}{\kappa}\right), \tag{1}$$

where κ is a parameter that determines the shape of the filter response function. Since this scheme is Gaussian in nature, then an "influence radius" R may be thought of as that radius where $w_m = e^{-1}$. It will be shown later that κ can be chosen to provide information in the analysis only at scales resolvable with a particular data distribution. The Barnes technique has gained wide acceptance in mesoscale analysis (e.g., Doswell, 1977; Maddox, 1980; Koch and McCarthy, 1982), because of this analogue of the weighting function to a simple Gaussian low-pass filter and the *a priori* determination of the response function.

When only one pass through the data is made, the spectral response [derived by Barnes (1964) upon the supposition that the data distribution can be represented by two-dimensional Fourier integrals] is

$$D_o = \exp\left[-\kappa_o\left(\frac{\pi}{\lambda}\right)^2\right] \tag{2}$$

as a function of horizontal wavelength λ. This yields an interpolated field given by

$$g_o(i, j) = f(x, y)D_o, \tag{3}$$

where $f(x, y)$ is an idealized monochromatic data field of the form $A \sin(2\pi x/\lambda)$. Figure 1 shows that use of smaller values of the dimensionless weight parameter $\kappa_o^* = \kappa_o/L^2$ results in greater filter response during the first pass, particularly for the short waves. Here L is an arbitrary scale length based upon the data distribution.

Barnes (1973) has modified the earlier (1964) version of his technique in order to decrease the amount of computer time necessary to achieve desired response at small wavelengths. This modification consists in applying only a single correction pass through (iteration upon) the initial interpolated field $g_o(i, j)$, rather than making several iterations as before. To accomplish this, parameter κ is decreased from its first pass value (κ_o) to a correction pass value of

$$\kappa_1 = \gamma\kappa_o, \tag{4}$$

by using a numerical convergence parameter $\gamma (0 < \gamma < 1)$ that forces a high degree of convergence (agreement) between the observation field $f(x, y)$ and the correction (second) pass interpolated field $g_1(x, y)$. Of course, it is not always desirable to have the interpolation field fit the data exactly. The analyst obtains the desired response following the second data pass by manipulating the value of γ.

The "correction (second) pass" grid field $g_1(i, j)$ is the result of adding to the first pass field the smoothed residual difference between the observed data values and the first pass estimated values "at" the data locations $g_o(x, y)$, or

$$g_1(i, j) = g_o(i, j) + [f(x, y) - g_o(x, y)]D_1, \tag{5}$$

where (after Barnes, 1973)

$$\begin{aligned} D_1 &= \exp[-\kappa_1(\pi/\lambda)^2] \\ &= \exp[-\gamma\kappa_o(\pi/\lambda)^2] \\ &= D_o^{\gamma} \end{aligned} \tag{6}$$

is the response function corresponding to the weight function

$$w'_m = \exp(-r_m^2/\gamma\kappa_o). \tag{7}$$

A simple bilinear interpolation between the values of $g_o(i, j)$ at the four surrounding grid points can be used to obtain an estimate for $g_o(x, y)$ at each data location. The actual correction pass value at each grid point is computed as the sum of the weighted averages from the two passes with M observations according to [after (5)]:

$$g_1(i, j) = \frac{\sum_{m=1}^{M} w_m f(x_m, y_m)}{\sum_{m=1}^{M} w_m} + \frac{\sum_{m=1}^{M} w'_m[f(x_m, y_m) - g_o(x_m, y_m)]}{\sum_{m=1}^{M} w'_m}. \tag{8}$$

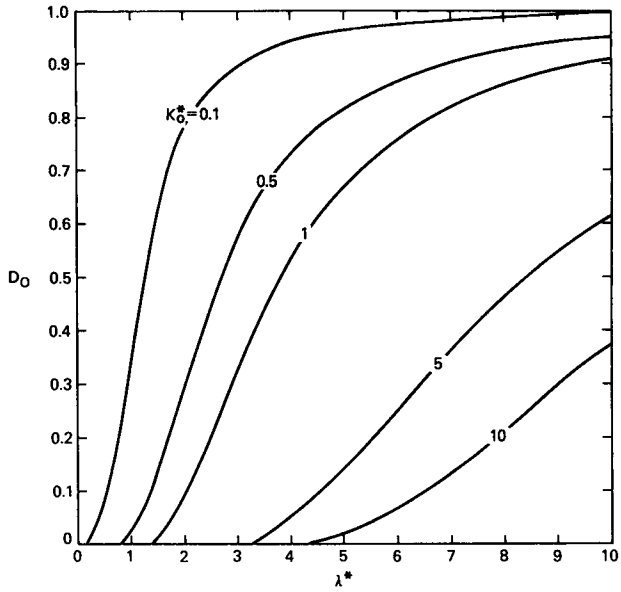

FIG. 1. Relationship of first pass response D_o to dimensionless wavelength $\lambda^* = \lambda/L$ for various values of dimensionless weight parameter $\kappa_o^* = \kappa_o/L^2$, in which L is an arbitrary scale length based upon the data distribution (e.g., $L = 2\Delta n$).

Since it follows from (5) that (omitting arguments for convenience)

$$D_1 = \frac{g_1 - g_o}{f - g_o}, \tag{9}$$

the function (6) might be referred to as a difference-field response function. The true correction pass response function [i.e., that one which corresponds to the first pass response function given by (2)] is

$$D_1^* = \frac{g_1}{f}, \tag{10a}$$

which upon substitution from (5) gives

$$D_1^* = D_o + (1 - D_o)D_1, \tag{10b}$$

and upon further substitution from (6) we have (Barnes, 1973)

$$D_1^* = D_o(1 + D_o^{\gamma-1} - D_o^{\gamma}). \tag{11}$$

The response function D_1^* is the proper measure of the degree of analysis convergence or, in other words, how closely the interpolated values agree with the observed ones after a second pass through the data. Making a second pass will increase the degree of convergence when $0 < \gamma < 1$, and particularly so when $\gamma < 0.5$. The amount of increase and the resulting final response are known *a priori* from (11). The greatest increase in response occurs at the shorter wavelengths.

A mathematical analysis of the effect of making additional passes ($N \geq 2$ iterations) through the data appears in the Appendix. It is proven there that no real benefit can be gained in making more than one correction pass becuse of the rapidity with which convergence is approached when γ is chosen small enough. It is also proven that the 1973 version of the Barnes objective analysis technique using the γ parameter is absolutely convergent [the 1964 version without use of γ has also been shown to be convergent (Barnes, 1964), though several more passes are required to reach the same degree of convergence as with the 1973 version]. This fact enables the analyst to control the amount of small-scale detail in the analyzed data fields.

Thus, an important reason for selecting the Barnes technique for interactive usage is that *only two passes through the data are required to achieve the desired scale resolution because of the rapidity with which convergence is reached.* Even when a large influence radius (weight factor κ) is chosen to reduce small-scale noise due to variations in observation density, convergence is still attainable.

Another desirable feature of the Barnes technique is that the weight function is not sensitive to whether or not a finite value is used for the cutoff radius R_c (beyond which all weights are assigned a value of exactly zero). By setting $R_c = \infty$, all the data in a given data set would be incorporated in determining each grid point value. However, for reasons of computational economics R_c may be set to some finite value as long as the value of the weight function at R_c is some very small number (i.e., so long as $R_c \gg R$). Since the weighting function decreases to zero asymptotically, the influence of data may be extended to any distance R_c to ensure that a sufficient number of observations influence each grid point value. Some care must be taken to ensure that R_c is sufficiently large that there be no noticeable effect upon either the weight function or the response characteristics.

It is of some interest to provide a comparison between the Barnes (1973) and Cressman (1959) objective analysis schemes, as they both are weighted-averaging techniques in common usage. One important difference concerns the choice of R_c. The Cressman weights do not asymptotically approach zero with increasing distance as they do in the Barnes technique, but instead abruptly become zero at $r_m = R_c$. This aspect of the Cressman scheme can present serious difficulties when the data distribution is non-uniform. In particular, those fields that havevery irregular data densities over the domain can present a problem termed ballooning, which is characterized by large amplitude and phase distortions in the neighborhood of any grid point whose value is determined primarily by the value of only one datum.

In general, this problem can be reduced by requiring that at least several observations be used in the calculation of each grid point value. In the Barnes technique, this is accomplished by extending the distance R_c (with no resulting effect upon the weight function). In some applications of the Cressman technique, the radius of influence is locally increased to ensure that a sufficient number of data influence each grid point value (Inman, 1970). However, noise introduced by such a locally varying weight function must be suppressed with additional numerical filters, thus producing an unknown final response and requiring additional computer time. Another correctional method sometimes applied with the Cressman technique is to increase the influence radius on the first pass throughout the entire domain. Yet such a procedure requires more passes to achieve the desired final response.

Classical sampling theory (Peterson and Middleton, 1963) dictates that a wave whose horizontal wavelength does not exceed at least twice the average observation spacing ($2\Delta n$) cannot be resolved since five data points are required to describe the wave and its derivatives. The Cressman (1959) and Barnes techniques both employ the method of successive corrections. Accordingly, an adjustment is made to the first pass analysis by decreasing the influence radius in the second pass through the data to restore the amplitude of small wavelength components larger than the $2\Delta n$ scale suppressed in the first interpolation-filtering pass. In the

Cressman case, neither the number of additional passes (typically 4–6) nor the value of the influence radius at the second pass are governed explicitly by the data distribution; thus, neither is the filter response. Stephens and Stitt (1970) show that an optimum choice for the Cressman influence radius on the first pass can be made in terms of Δn for a uniform data distribution. However, the optimum influence radius is not well-known theoretically on additional passes, so the final filter response is rather arbitrary. Random errors in the observations generate fictitious $2\Delta n$ waves (Barnes, 1964). Therefore, it is desirable to filter these from the analysis as much as possible. It will be shown later that the Barnes filter response characteristics can be determined prior to the analysis so that pattern scales resolvable by the data distribution will be revealed to a known degree.

3. The Barnes scheme tailored to GEMPAK needs

The GEMPAK version of the Barnes scheme includes the following features:

1) Specific kinds of data and grid domains are used to permit easy manipulation of data file structures and to obtain a uniformly reliable analysis throughout the entire grid area displayed.

2) Differences in the nature of conventional and satellite data are accounted for. In particular, satellite data tend to occur in clumps or swaths separated by varying distances. Two different data spacings are calculated from the given data set to inform the user when clustering is significant. This is needed because the Barnes scheme assumes uniform distribution of data.

3) The maximum allowable detail in the interpolated fields is governed by the data spacing (in that the $2\Delta n$ wave is filtered from the analysis). The weights are calculated internally as a sole function of the data spacing.

4) The results of the mathematical analysis of the Barnes convergence properties (Appendix) are incorporated by making two passes through the data.

5) Bounds to the grid spacing are uniquely determined by the data spacing. Since the magnitude of derivative fields like divergence and vorticity is highly sensitive to grid size, then this size must be justified on theoretical grounds.

6) Measures of analysis quality are made available to the analyst to allow objective determination of the effect of the analyst's manipulation of the analysis filter control parameters upon the resulting objective analysis, and to assure the analyst that a sufficient number of observations influence each grid point value.

7) The interactive Barnes scheme can easily be used by one who does not possess an understanding of the theoretical aspects of the scheme, but who does have the ability to judge the quality of the resulting objective analysis in terms of its physical content, consistency with other meteorological fields, and temporal continuity. A minimum of human intervention is necessary. Analyses can be produced and displayed at the rate of one every 2 min once the input parameters have been decided upon.

These features provide for a reasonable balance between manipulation and objectivity. The details of each of these features are now discussed.

a. Domain definitions

A common problem in conducting a numerical map analysis is that errors are introduced by extrapolating observed values to typically data sparse regions near the edges of a data region. The Barnes scheme is not immune to this problem. To help prevent this, specific domain definitions are used in the interactive scheme (Fig. 2). One of these domains is termed the data file, which consists of the entire data set to be tentatively considered for the Barnes objective analysis. The subset of the data file in which grid point values are actually computed from the data by the interactive scheme is termed the data area. Those observations which lie outside of the data area do not influence any grid point value. A kind of data area frequently considered is one in which the distribution of the data is more uniform than that within the data file (as shown). The grid display area is that portion of the entire gridded domain (i.e., data area) which is displayed as "the objective analysis" to the analyst. The grid display area should lie entirely within the data area to avoid attempted interpretation of the analysis near the data-sparse boundaries of the data area (the dashed region). If the grid display area were allowed to cover the entire data area, the data would be simply extrapolated by the Barnes scheme because there are not enough data nearby to give reliable grid

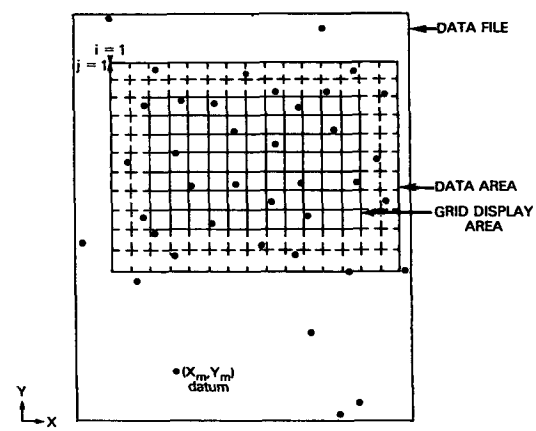

FIG. 2. Schematic illustration of data and mesh domains used within the interactive Barnes scheme.

point estimates. A good approach to take is to have at least one or two observations within the data area remain beyond each side of the grid display area. This is almost always possible even with satellite data sets composed of highly non-uniformly spaced observations.

b. *Non-uniform data distributions*

The problem of handling non-uniform distributions within the data area is dealt with in the following manner. First, the distance between each observation and its nearest neighbor is determined. The average of these distances over the entire data area is termed the computed data spacing, Δn_c. Its value determines the maximum detail permitted in the objective analysis. Then, a smoother analysis can be obtained by manually inputing any $\Delta n > \Delta n_c$. This should be done, for example, when examining the synoptic-scale impact of clustered mesoscale satellite data upon a field of synoptic-scale conventional data. An appropriate choice in this case is the Δn computed from the data area comprised only of the conventional data. In other words, the purpose of the analysis should govern the choice for Δn, under the constraint that $\Delta n \geq \Delta n_c$.

When the data spacing is severely non-uniform, another computed data spacing called the "random data spacing" can be used as a guide. The value of Δn_r represents what the average data spacing would be inside a square data area A if M observations were uniformly distributed across the area. If the data set is severely clustered, then Δn_r will greatly exceed Δn_c. Effectively Δn_r can be used as a simple guide for determining which data spacing larger than Δn_c to employ:

$$\Delta n_r = A^{1/2}[(1 + M^{1/2})/(M - 1)]. \qquad (12)$$

c. *Control of detail in a two-pass Barnes analysis*

Once the data spacing has been defined, the analyst "fine tunes" the degree of analysis detail (or convergence of the interpolated field towards the observed field) by choosing a value for the numerical convergence parameter (γ). In the interactive Barnes scheme, the maximum detail is obtainable with $\gamma = 0.2$, whereas the least detail results with $\gamma = 1.0$, for a given value of Δn. The analyst must decide how closely the final analysis should be forced to fit the data. It is justifiable to use a small γ value only when errors in the data are a small fraction of the signal present over the field and when the observations are not substantially contaminated by subgrid-scale atmospheric processes. The degree of spatial uniformity of the data is an additional factor that can enter into this decision. The important thing here is that the interactive Barnes scheme only imposes an upper limit on the amount of resolvable detail.

Under the two-phase constraint and the further constraint that $0.2 \leq \gamma \leq 1.0$, the range of permissible responses can be found for the value of Δn used (Fig. 3). The first pass value of the response function D_o as a function of wavelength is arrived at by choosing an appropriate value for $D_o(2\Delta n)$ and calculating $D_o(\lambda)$ from (A18). The second pass values $D_1^*(\lambda)$ are then calculated from (11). The value of 0.0064 for $D_o(2\Delta n)$ is selected to give a second pass response of $D_1^* = e^{-1}$ at the $2\Delta n$ wavelength when $\gamma = 0.2$. Since in the GEMPAK Barnes scheme the maximum response and best fidelity characteristics of the scheme's inherent low-pass filter are arrived at by choosing this γ value, use of $D_o(2\Delta n) = 0.0064$ lets us obtain a baseline value by which responses at multiples of the $2\Delta n$ wave can be calculated. It is important to realize that under these conditions, the weight parameter κ_o is fixed by the data spacing, since when $\lambda = 2\Delta n$ is inserted into (2) with $D_o(2\Delta n) = 0.0064$,

$$\kappa_o = -\left(\frac{2\Delta n}{\pi}\right)^2 \ln D_o(2\Delta n)$$

$$= 5.052\left(\frac{2\Delta n}{\pi}\right)^2. \qquad (13)$$

In other words, the weight parameter κ_o is fixed by the data spacing to give maximum response of no

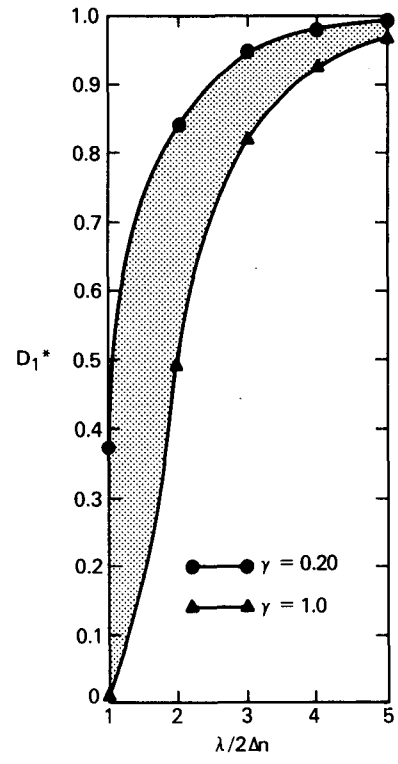

FIG. 3. Permissible second (correction) pass filter responses as functions of multiples of the $2\Delta n$ wavelength in the interactive Barnes scheme.

more than e^{-1} at the $2\Delta n$ scale ($\gamma = 0.2$). The analyst has the option of either accepting this default analysis or of making a smoother, less detailed one by selecting a larger γ value ($0.2 \leq \gamma \leq 1.0$).

d. Objective determination of grid size

Typical bounds on the ratio between the grid spacing Δx and the data spacing Δn appear to lie in the range of ~0.3–0.5 (Barnes, 1964, 1973; Doswell, 1977; Maddox, 1980; Koch and McCarthy, 1982). There are sound reasons underlying these empirical findings. Since five grid points are required to represent a wave (Peterson and Middleton, 1963) on a grid, and the minimum resolvable wave is of $2\Delta n$ scale, then Δx must be no larger than one-half of Δn to guarantee proper representation of resolvable wavelengths (as shown in Fig. 4). As for the lower limit, it is widely understood that calculations of derivative quantities like divergence and vorticity are highly sensitive to grid length. An unrealistically noisy derivative field may result when the grid is too fine. Therefore, if such derivative fields are to represent only resolvable features, a grid length should be chosen that is not much smaller than the data spacing. For these reasons, the interactive GEMPAK Barnes scheme imposes the constraint that $\frac{1}{3} \leq \Delta x/\Delta n \leq \frac{1}{2}$.

Even though the scheme places stringent limits on the mesh size, it remains versatile enough that it can accommodate round-off of the computed mesh size to convenient whole numbers (1.0 deg latitude, 10.0 km, etc.). This versatility may be necessary when making comparisons of objectively analyzed data to numerical model output, for instance.

e. Quality control indicators

A measure of analysis quality is the field-averaged rms difference (rmsd) between the interpolated and observed fields. This number is displayed to the analyst after both the first and second passes through the data to show how the amount of rms reduction between passes varies with the chosen γ values. The rmsd can then be compared to known observational errors to help the analyst decide upon how much smoothing to accept in the final product.

Another useful quality control indicator is a display of the degree to which the individual interpolated values have converged to the observed data values. The scheme can, if desired, be asked to interpolate the grid point values $g_1(i, j)$ back to the data locations and to calculate the difference between the $g_1(x, y)$ and the data $f(x, y)$ fields. Then, one can either display these interpolation differences at those locations or do an objective analysis of the differences. The latter option allows the analyst to easily visualize patterns in interpolation-related rmsd. It will be shown in several examples in the next section how such information can be extremely useful when one merges data sets with different characteristics. It is also helpful to examine the rmsd field when the data are nonuniformly distributed across the data area, and when there is concern about the choice of grid display area and boundary effects.

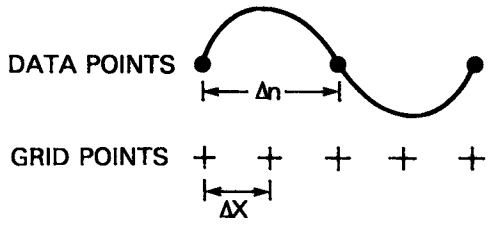

FIG. 4. Determining the proper relationship between grid size and data spacing from elementary considerations.

As discussed earlier, serious "ballooning" problems can occur when an insufficiently small number of data determine the value at a grid point. In order to avoid such problems, a warning flag appears to the analyst whenever less than three datum determine the value of any grid point ($M = 3$ is the result of empirical tests with the scheme). Such a problem is most likely to occur when the grid display area is chosen so large that it extends into data-void regions. It is desirable to caution the analyst that a better choice for the grid display area should have been made.

The warning flag appears, in effect, because the cutoff radius R_c (see Section 2) is finite. There may be some grid points which are not influenced by at least three datum whenever the data distribution is extremely clustered, or when the grid display area is chosen too large so that it extends beyond the area in which the data can exert much influence on grid point values. It is important to maintain a large but finite value for R_c to warn the analyst of clustering or domain choice problems. The cutoff radius has the additional practical benefit of increasing the speed of weight calculations (by eliminating calculation of extremely small weights), without noticeably deteriorating the quality of the analysis. We employ $R_c = (20\kappa_o)^{1/2}$ at which distance $R_c/R = 4.5$ and the actual weight value would be $w_m = 2 \times 10^{-9}$ [from (1)]. In terms of grid spacing when $\Delta x = \Delta n/2$, it follows from (13) that $R_c/\Delta x = 12.8$. Thus, R_c is chosen sufficiently large that the filter response characteristics remain virtually unaffected.

f. Balance between versatility and objectivity

The GEMPAK Barnes scheme is a versatile, easy-to-use, practical objective analysis package. Its versatility lies in its acceptance of user inputs to data area, grid display area, data spacing, grid spacing, and the numerical convergence parameter γ.

The scheme maintains objectivity:

1) through the limits internally imposed on the value of γ ($0.2 \leq \gamma \leq 1.0$), the number of passes

through the data (2), and constraints on both $\Delta x(\Delta n/3 \leqslant \Delta x \leqslant \Delta n/2)$ and $\Delta n(\Delta n \geqslant \Delta n_c)$,

2) as a result of the fact that the weights are determined solely by Δn and calculated internally so that the $2\Delta n$ wave is effectively removed from the analysis according to (13).

The scheme remains practical and easy because:

1) an interactive, question-and-answer type format and various cursor/display controls on AOIPS are employed to permit the analyst to quickly visualize selected data or grid domains and the effect of variations in the values of the analysis control parameters on the analysis;

2) human manipulation is minimized;

3) quality control indicators speed the analyst's decision-making activities;

4) the same calculated weights can be applied to many different parameter fields as long as the data quality and distribution do not vary appreciably.

The last statement raises some interesting points. Since the most time-consuming part of the objective analysis is the computation of exponentials, large grids or data areas containing a large number of stations will limit the number of parameters that can be analyzed at one time. The number of exponentials computed is approximately $N \doteq 2(M)(KX)(KY)$, where M is the number of observations and KX and KY are the number of grid points in the x and y directions. Since N is not a function of the number of parameters being analyzed, it has been found most efficient to compute as many parameters as possible during a single analysis. In the most recent version of the GEMPAK Barnes scheme, the exponentials are being saved as a file to reduce CPU time.

The effect that use of the same exponentials on different meteorological variables has upon the analysis of the variables should be clarified. All variables observed within a network are analyzed with an identical set of weights, because the weight values in this scheme are solely determined by the distances between grid points and observation points. However, this does not mean that the analyses will appear similar, nor that the temporal and spatial spectra of the variables will be identical. The weights only affect the degree of spatial smoothing. Thus, only the high frequency cutoff and the resulting spectral slope of the spatial spectra would be affected by the objective analysis-interpolation process when multiple use is made of a given set of weights.

4. Meteorological applications of the GEMPAK Barnes scheme

In this section, the input parameters which allow the analyst to interactively tailor the analysis of data sets to his or her specific needs are each varied to illustrate the effects upon the objective analyses. Three data sets are analyzed in this regard:

1) An almost uniformly distributed data set derived from the SESAME regional-scale rawinsonde network. An analysis is made of the wind speeds at the 310 K isentropic surface at 2100 GMT 10 April 1979. This data file, consisting of 32 of the 42 stations comprising this network, will be called SESAME RAWIN.

2) A highly clustered, non-uniformly distributed data set consisting of wind speeds reported at the 825 mb level of the SESAME regional-scale rawinsondes, combined with satellite-derived-motions of tracked low-level clouds. This combined wind data set, collected at 1800 GMT 10 April 1979, constitutes the data file to be called SESAME CLOUDWIND.

3) A totally satellite-derived data set with intermediate degree of non-uniformity consisting of temperatures derived from the VAS radiance measurements. This data file, known here as VAS TEMP, consists of temperatures assumed representative of conditions at 920 mb over the central part of the United States at 1202 GMT 20 July 1981.

In all of these analyses, the first task is to display a map of the observations within the data file, plus an additional data-free area of 1–3° latitude/longitude to facilitate map display. Once the map has been generated, the vertical level, data set name, data and grid display areas, etc., are entered. The domain areas can be positioned visually by using a video cursor, or by determining the appropriate coordinates of the lower-left and upper-right corners of the area and then entering these values on the terminal console.

a. Effect of parameter variations upon analysis of the SESAME RAWIN data file

A comparison of two GEMPAK Barnes analyses of the SESAME RAWIN data file generated by 1) having the grid display area smaller than the data area (Fig. 5a) and by 2) having the two areas equal (Fig. 5b), demonstrates the rationale behind choosing the former option. A less reliable analysis results when the data and grid display areas coincide, especially near the eastern and southern sides of the box. Notice that the observations at Nashville, Tennessee and those throughout southern Texas are not incorporated into that analysis, resulting in loss of valuable information on the strong wind speed gradients actually there. By comparison, the analysis displayed in Fig. 5a was generated from grid points, each of which have been influenced by values at station locations which totally surround it.

In both of these analyses, the numerical convergence parameter γ was assigned a value of 0.3. Anal-

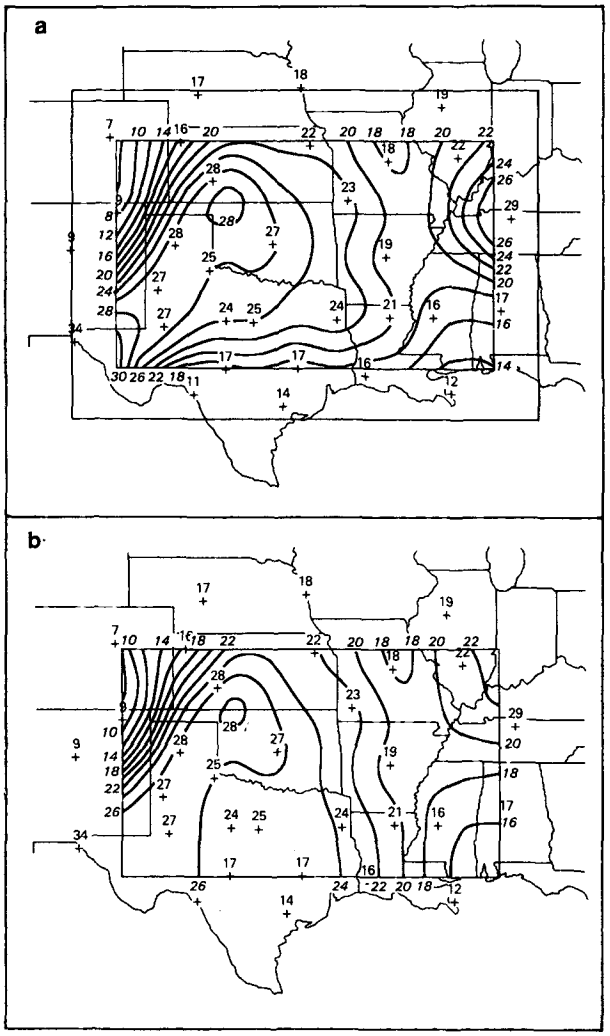

FIG. 5. Two analyses of the SESAME RAWIN data file (isotachs in m s^{-1}). Analysis generated by having (a) grid display area nested 2.0° within the 22 × 14 data area and (b) the two areas are coincident. Both analyses are based on using Δn = 2.0°, Δx = 1.0°, and γ = 0.3. Data values are shown above station locations denoted by crosses.

yses of the SESAME RAWIN data file with four different values of γ (0.2, 0.3, 0.5, and 1.0) are displayed in Fig. 6. The analysis produced with γ = 0.2 exhibits noticeable detail at the $2\Delta n_c$ scale. Larger values of γ lower the response to that scale [as given by (11) and Fig. 3] and accordingly dampen the analysis detail.

The analyst must judge which value of γ produces the best analysis for his or her purposes. There are several tools available to the analyst within this interactive scheme to help in this decision. First, the rmsd (rms difference between the interpolated and observed fields) should be no larger than the estimated rms error (rmse) in the observations. Since errors are additive, it would be most desirable to keep the rmsd introduced by the analysis scheme considerably below the rmse of the original observations. The computed rmsd can help serve as an upper limit on the choice of γ. Second, the meteorological features appearing in the analyses should exhibit acceptable temporal and spatial continuity. The lower limit on γ is determined by the continuity considerations, which is best made by examining derivative fields like divergence and vorticity. Third, the analyst should examine the interpolated fields resulting from the largest γ value first, and then reduce γ in steps until an unacceptably small signal-to-noise ratio becomes evident.

Application of the rms quality criterion to the objectively analyzed wind speed fields is illustrated. An observational rmse of 3–6 m s^{-1} can be expected for winds between the 700 and 400 mb pressure surfaces (Fuelberg, 1974), through which the 310 K isentrope passes in this case. The analysis rmsd, averaged over the grid display area, exceeds 1.5 m s^{-1} only for values of $\gamma \geq 0.5$. Thus, the γ = 0.2 or γ = 0.3 analysis would be preferred upon this basis.

The spatial distribution of the rmsd (interpolation differences) as a function of the value chosen for γ is presented in Fig. 7. The maximum differences are generally reduced by a factor of 2 when γ is decreased from 1.0 to 0.3. This result is consistent with the fact that the analysis converges more to the observational field (shows more detail) as γ is reduced. A display such as this enables the analyst to see that the greatest differences occur 1) where gradients are strongest (in eastern New Mexico and western Kansas), in that the true magnitude of the gradient is underestimated, 2) where there is small-scale variability (in Fig. 7b along the Red River in northern Texas) and 3) generally when γ is largest. This kind of display can greatly facilitate interpretation of the analysis.

For this data set, the computed value of the data spacing is Δn_c = 1.93° and the random data spacing is Δn_r = 2.49°. Thus, the data distribution is nearly uniform. For convenience in incrementing the size of the domain areas in steps of Δx, the analyst input a data spacing of Δn = 2.00° and a grid spacing of Δx = 1.00°. The bounds of Δx allowed by the scheme for this data file are 0.65° ($\Delta n/3$) and 1.00° ($\Delta n/2$). An objective analysis (not shown) was made using Δx = 0.65° with no perceptible difference in the analysis. The Δx limits in the scheme are designed to achieve a convenient round number with which to work and not to attempt the control of detail in the objective analysis.

b. *Analysis of non-uniformly distributed data in* SESAME CLOUDWIND *data file*

A comparison is made in Fig. 8 between an objective analysis of SESAME rawinsonde winds at 825 mb at 1800 GMT 10 April 1979 and an objective analysis of the same winds combined with non-uniformly dis-

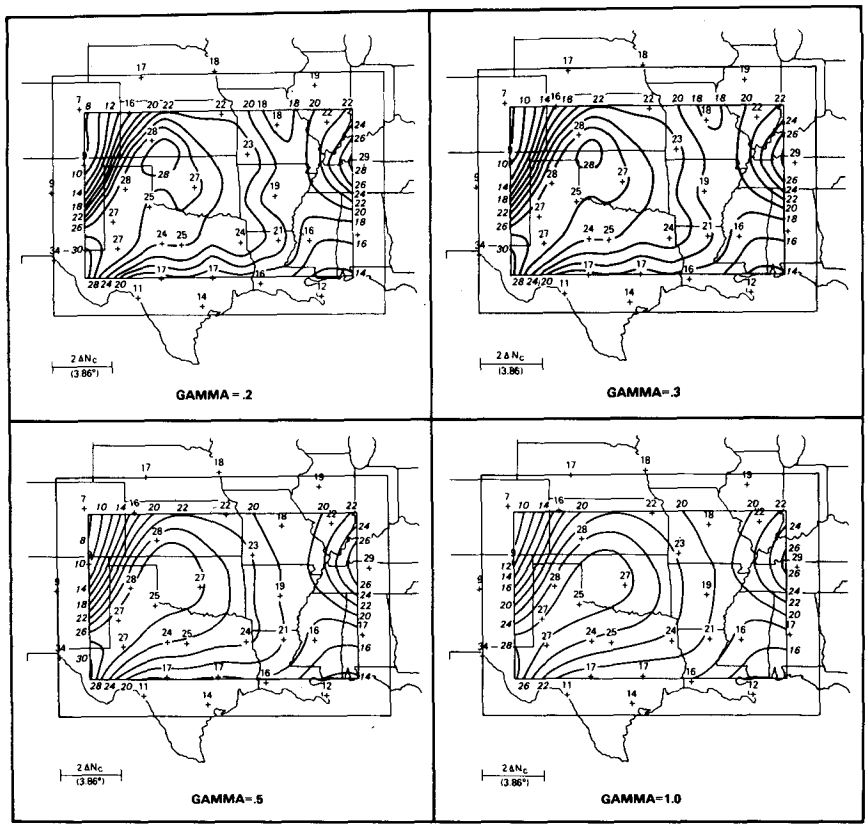

FIG. 6. Changes in the objective analysis of the SESAME RAWIN data set brought about by variations in the value input for γ (analysis with $\gamma = 0.3$ is identical to that in Fig. 5a).

tributed satellite data (the SESAME CLOUDWIND data file). These analyses are being used in a continuing investigation at NASA/GLAS to determine to what extent assignment of the cloud motion vectors to an incorrect height will degrade a conventional analysis of winds at the SESAME regional scale (Peslen *et al.*,

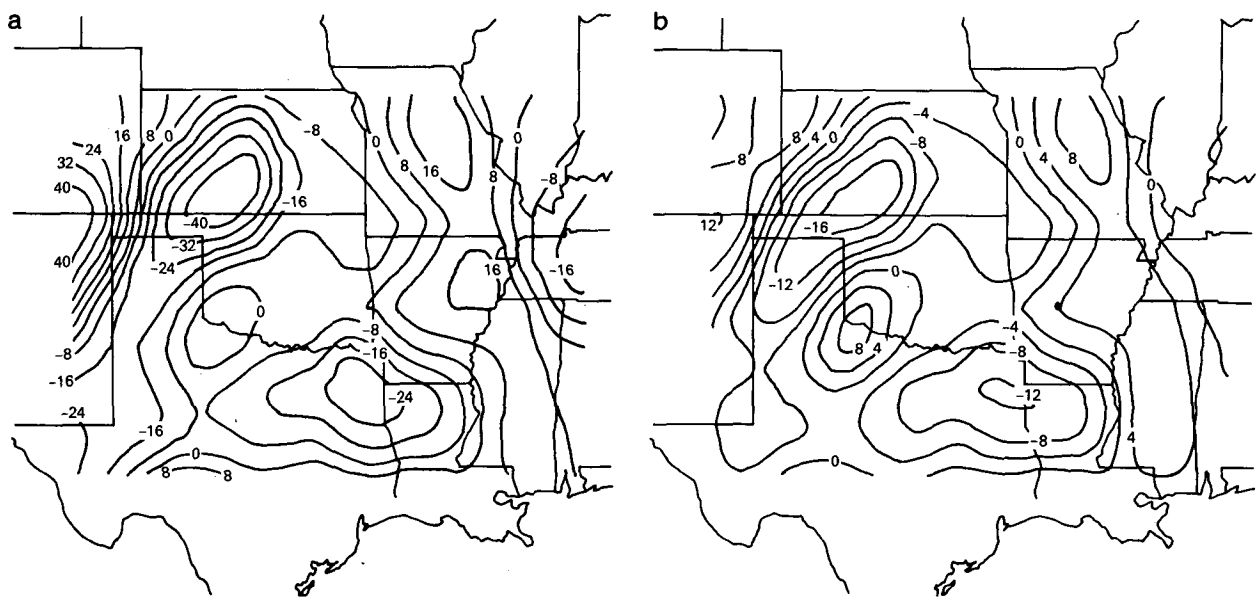

FIG. 7. Objective analysis of interpolation differences (rmsd) for (a) $\gamma = 1.0$ and (b) $\gamma = 0.3$ analyses as depicted in Fig. 6. Contours are isotachs at intervals of 10^{-1} m s^{-1}.

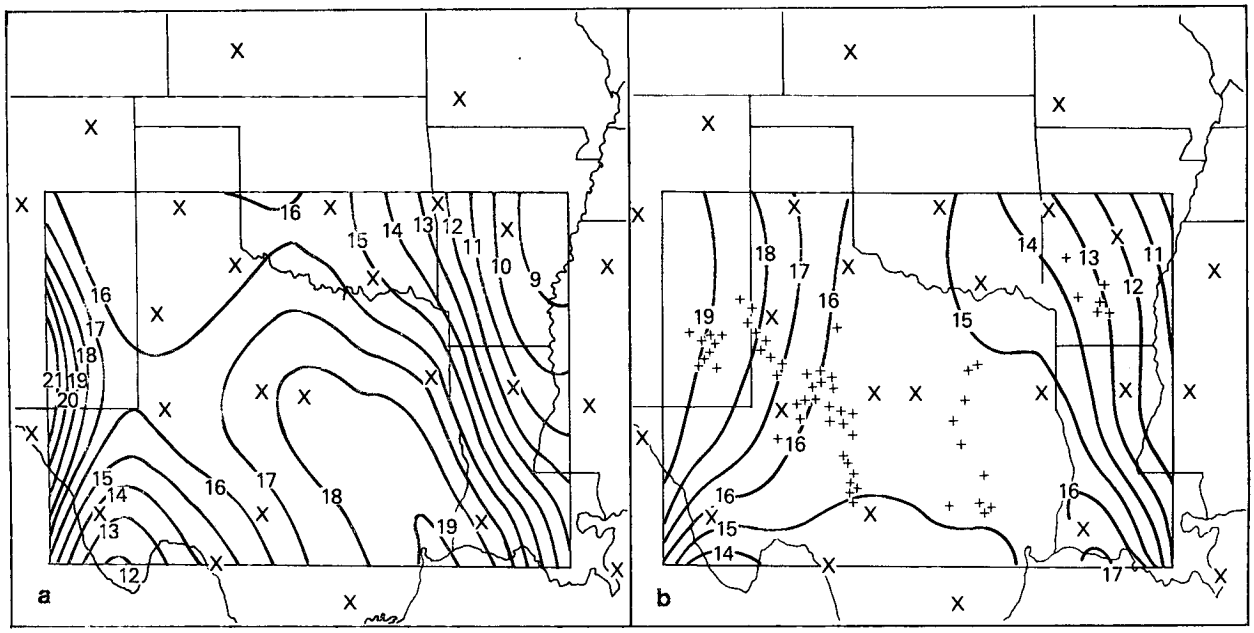

FIG. 8. Objective analyses of (a) nearly uniformly distributed and (b) highly non-uniformly distributed wind data sets. Data spacing in (b) analysis (of SESAME CLOUDWIND data) is set equal to that in the (a) analysis (of SESAME rawinsonde data). Input parameter values used were $\Delta n = 2.0°$, $\Delta x = 1.0°$, and $\gamma = 0.3$. Both analyses utilize data at 825 mb for 1800 GMT 10 April 1979.

1982). With this purpose in mind, the grid display area is adjusted to just barely cover the area of satellite data. Likewise, for this purpose, the value of Δn input to the computer is that of the uniformly distributed, conventional rawinsonde data at the SESAME regional scale ($\Delta n = 2.00°$), rather than the computed minimum observation spacing Δn_c, which has a much smaller value (0.69°) because of the small distances between adjacent satellite observations.

Clearly, the satellite data exert an impact upon the conventional wind analysis on scales resolvable by the SESAME regional rawinsonde network. At least part of the difference between the two analyses can be explained by a systematic (rawinsonde scale) misassignment of all the cloud vectors to one isobaric level, when in actuality the clouds exist at different heights above the local terrain (Peslen *et al.*, 1982). The problem of misassignment of heights is most crucial in a vertically sheared environment.

The rmsd interpolation difference map for the SESAME CLOUDWIND analysis (Fig. 8b) appears in Fig. 9. The differences are all smaller than 1.0 m s^{-1} except in two small areas near the southern edge of the grid display area. In fact, over most of the analyzed area, differences are no larger than 0.5 m s^{-1}, which is quite acceptable. The small "balloons" over southern Louisiana and southwestern Texas are due to extrapolation of values from the rawinsonde stations to grid points in the data-void regions beyond the grid display area. These two features could have been avoided by slightly reducing the size of the grid display area. However, it is not necessary as long as their existence is recognized in interpreting the objective analysis. It should be clear that the analysis quality control factors neither measure directly nor allude to the presence of systematic errors in the data. Systematic misassignment of cloud heights and the systematic effects of vertical wind shear on

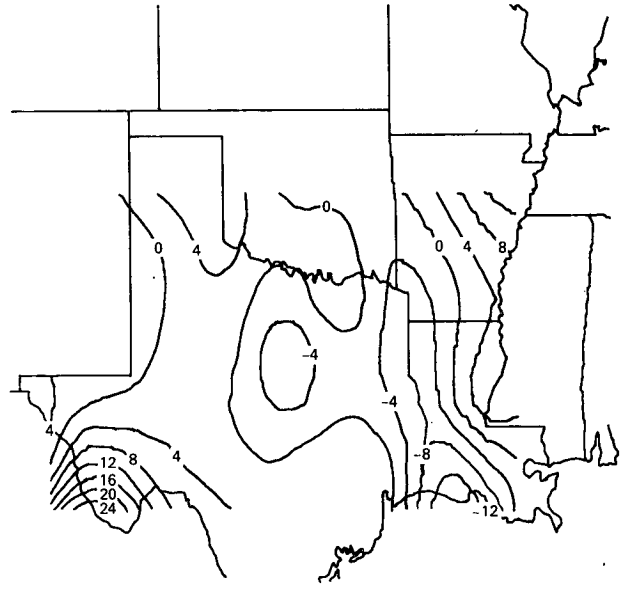

FIG. 9. Objective analysis of interpolation differences resulting from analysis in Fig. 8b (isotachs at intervals of 10^{-1} m s^{-1}).

satellite cloud wind data sets are recognized problems (Peslen *et al.*, 1982) which must be dealt with prior to conducting the objective analysis.

c. *Maintenance of smooth gradients in data-void areas in* VAS *data file*

An analysis of the VAS TEMP data file appears in Fig. 10. This data set is not as severely clustered as is the SESAME CLOUDWIND data set. Yet, large data gaps like those in Nebraska and Kansas are evident. This problem is perhaps made worse because significant gradients might be anticipated there (visual interpolation from the data locations to the gap areas). The VAS data would appear with a regular spacing were it not for the presence of clouds or data collection problems at some points (Chesters *et al.*, 1982). In this case, $\Delta n_c = 0.82°$ and $\Delta n_r = 1.13°$ were computed by the scheme. For convenience, the analyst input $\Delta n = 1.0°$ and $\Delta x = 0.5°$. In this case, the GEMPAK Barnes scheme has been able to maintain smooth gradients in the data-void regions. Furthermore, the interpolation difference analysis (Fig. 11) shows that the small-scale variability in the data (notably in Missouri) has been smoothed out. Notice that such questionable data values as the 27°C value in eastern Missouri have little influence upon the resulting analysis. This smoothing of noise introduced by data errors is a characteristic of all objective analysis schemes. Such displays as these allow the analyst to determine the extent of this smoothing.

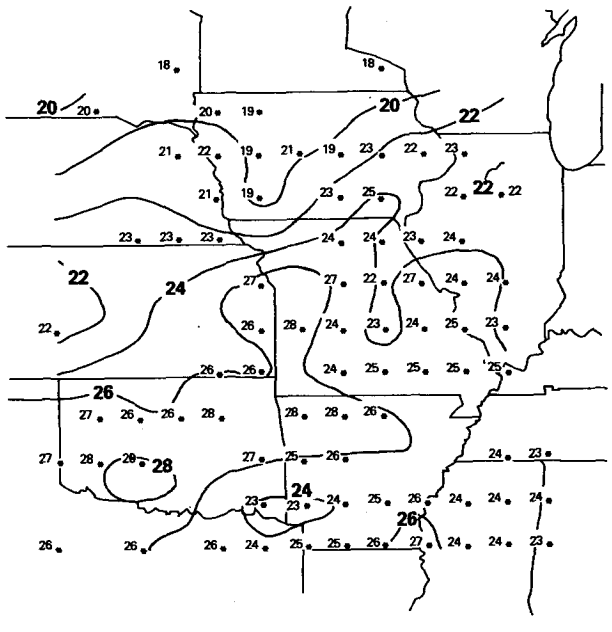

FIG. 10. GEMPAK Barnes analysis of the VAS TEMP data file (isotherms at 2°C intervals). Data values shown at locations denoted by an asterisk.

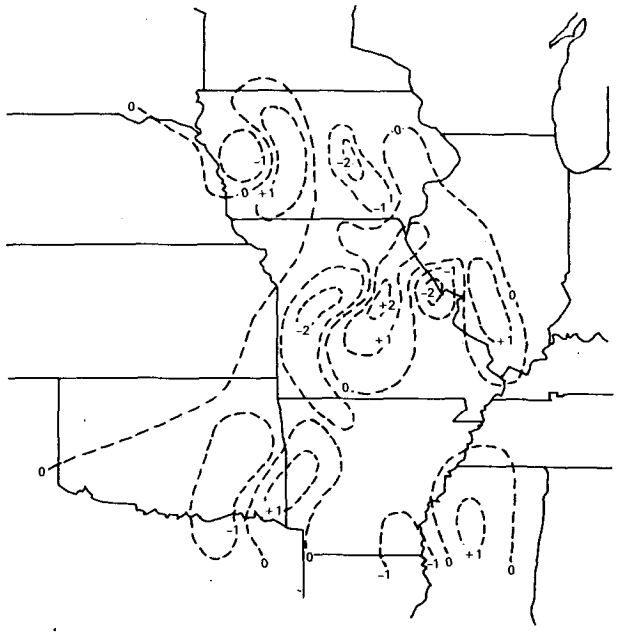

FIG. 11. GEMPAK Barnes analysis of the interpolation difference field (°C) corresponding to Fig. 10.

5. Summary

An interactive Barnes (1973) objective analysis scheme has been implemented as part of the GEMPAK interactive analysis package on the AOIPS data processing system. The scheme is specifically tailored to the needs of the research meteorologist to quickly assess the impact of satellite-derived data on analyses of conventional meteorological data sets. It allows the analyst to modify the values of input parameters used in the objective analysis within objectively determined, internally set limits and to quickly see the effect of such manipulations upon the analysis. Special features include methods for dealing with the spatially clustered nature of satellite data and with the different horizontal resolutions of the various data types.

The Barnes scheme was selected for implementation on an interactive computer because it is computationally efficient with filter response characteristics that are known functions of the data distribution. It is proven here that the scheme adequately recovers details after only two passes through the data even when a large influence radius is used to ensure that sufficient data influence is exerted at all grid points.

The interactive Barnes scheme incorporates several objective constraints on the analysis over which the analyst has no control, while still providing some user input via an interactive computer video terminal. The various features that make the scheme objective, versatile, and practical are summarized in Fig. 12.

Three data sets were analyzed to illustrate these

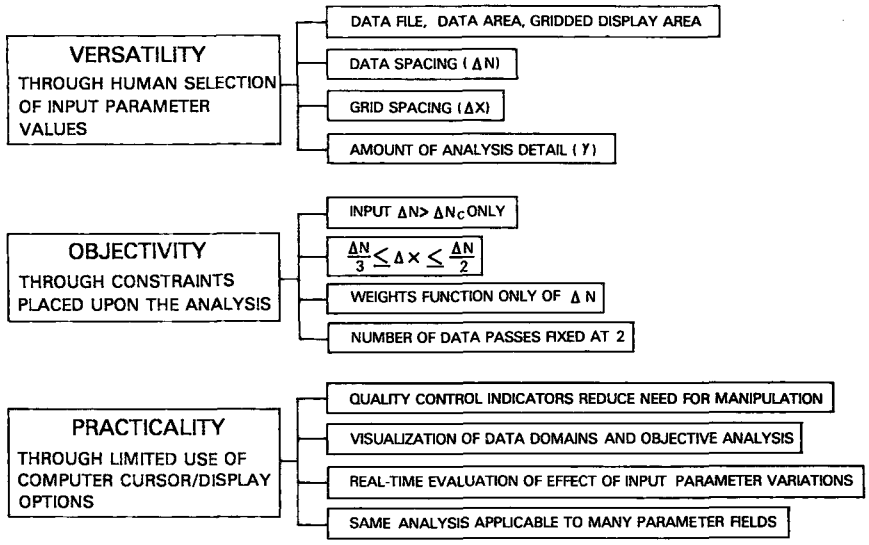

FIG. 12. A summary description of the unique features of the GEMPAK Barnes scheme.

characteristics. The first, that of a SESAME rawinsonde wind data set with nearly uniform spatial distribution, was one in which the data spacing used in the analysis was the value calculated by taking the average of the distance between each datum and its closest neighbor (Δn_c) over the entire data area. This resulted in filtering the $2\Delta n_c$ wave from the gridded fields. Use of the quality control displays helped the analyst determine how much smoothing was justified.

In the second case, a data set composed of satellite-derived cloud motions combined with SESAME rawinsonde winds was studied. The resultant data file was characterized by severe clustering of data. Use of Δn_c was judged inappropriate in this case, because the smallest scale at which such satellite data provide real information is presently unknown. The interactive scheme permitted the analyst to input a larger effective data spacing than the calculated one, namely, that calculated from the rawinsonde network only, with the result that a less detailed analysis was made. The scheme imposes an upper limit on the maximum amount of detail that can be resolved with a given data set.

The third data set, that of VAS-derived temperatures, was characterized by an intermediate degree of spatial non-uniformity and large data gaps. This data set was chosen to demonstrate the capability of the scheme to produce realistic gradients in otherwise data-void regions and to filter out suspected gross data errors. Thus, the analyst could assess the quality of both the data and the analysis in real time. Of course, it is advisable first to subject the data to quality control procedures to remove gross systematic errors before the step of objective analysis is taken, since no variation of the input parameter values can remedy that problem.

6. Future plans

Several modifications to the GEMPAK Barnes scheme are both anticipated and possible with present AOIPS computer resources. One highly desirable addition to the present package is a comprehensive, automated, interactive data editing/quality control routine that would allow the analyst to selectively alter or omit troublesome observations. Displays of data time series, time tendencies, map plots, hydrostatic and superadiabatic checks, etc., are envisioned for this addition.

Work is being conducted to determine more objectively what data spacing to use with non-uniformly distributed data sets. It is likely that the optimum spacing will be a function of the representativeness, or error magnitude, characteristic of the particular data type as well as the nature or degree of non-uniformity of the data distribution (Maddox and Vonder Haar, 1979). It is also possible that a first-guess field provided by a mesoscale numerical weather prediction model could be used to replace the first pass through the data field.

Acknowledgments. Dr. Louis Uccellini originally suggested the task of adapting the Barnes scheme to meet the specific requirements of GEMPAK and he also offered improvements to this report. Additional suggestions made by Dr. Stanley Barnes (NOAA/ERL/OWR) and Dr. Joanne Simpson during their review of the manuscript have been incorporated herein. Cynthia Peslen kindly provided the satellite-derived wind data set and permitted presentation of the objectively analyzed fields. Thanks are also extended to Keith Brill of General Software Corporation who assisted in the analysis of the convergence properties of the Barnes scheme.

APPENDIX

Convergence Proof and Discussion

The mathematical–numerical analysis presented here shows that the Barnes (1973) scheme is absolutely convergent, but that no significant improvement in filter response fidelity (steepness of response curve) is obtained by making more than two passes through the data when γ is chosen sufficiently small. It is concluded that only one correction pass is sufficient to achieve acceptable analysis convergence at resolvable wavelengths.

1. Convergence proof

Convergence in an absolute sense occurs when the difference between the observed and analyzed data fields vanishes as the number of passes through the data approaches infinity, or stated mathematically

$$\lim_{N\to\infty}[f(x, y) - g_N(x, y)] = 0, \tag{A1}$$

where $g_N(x, y)$ is the interpolated field obtained after N iterations ($N + 1$ passes). It was shown in the text that a single application of the reduced weight parameter $\kappa_1(4)$ upon the weight function $w_m(1)$ results in the true response function $D_1^*(11)$ and the difference field response function $D_1(6)$ at the second (correction) pass. Weight functions at additional passes using successively decreasing values of κ_N, assuming that γ is kept constant through all passes, are defined by

$$\kappa_N = \gamma\kappa_{N-1} = \gamma^N\kappa_o. \tag{A2}$$

Application of these additional filter functions results in difference response functions at each pass given by

$$D_N = D_o^{\gamma^N}. \tag{A3}$$

When the value chosen for γ is less than unity, the response is further accentuated at each additional pass, particularly at short wavelengths where the initial response D_o is small.

It follows from the expression for g_1 in (5) that the third pass ($N = 2$) interpolated field is

$$g_2 = g_1 + (f - g_1)D_2, \tag{A4}$$

or upon further substitution that

$$g_2 = g_o + (f - g_o)[D_1 + D_2(1 - D_1)]. \tag{A5}$$

Following this procedure a step further, one can easily show that on the fourth pass

$$\begin{aligned} g_3 &= g_2 + (f - g_2)D_3 \\ &= g_o + (f - g_o)[D_1 + D_2(1 - D_1) \\ &\qquad + D_3(1 - D_2)(1 - D_1)]. \end{aligned} \tag{A6}$$

Accordingly, the general form of the equation describing the Nth pass interpolated field is

$$g_N = g_o + (f - g_o) \times \{D_1 + \sum_{i=2}^{N}[D_i \prod_{j=2}^{i}(1 - D_{j-1})]\}. \tag{A7}$$

To obtain the condition for convergence, this equation is substituted into (A1), resulting in

$$\lim_{N\to\infty}(f - g_o) \times \langle 1 - \{D_1 + \sum_{i=2}^{N}[D_i \prod_{j=2}^{i}(1 - D_{j-1})]\}\rangle = 0. \tag{A8}$$

Finally, because $(f - g_o)$ is a fixed constant, convergence is attained when

$$\psi_N = 1 - D_1, \tag{A9}$$

where D_1 is given by (6) and

$$\psi_N = \sum_{i=2}^{N}[D_i \prod_{j=2}^{i}(1 - D_{j-1})], \quad 2 \leqslant N \leqslant \infty. \tag{A10}$$

Before proceeding with the analysis of the convergence criterion, one should understand the relationship between it and the actual response function at the Nth iterative pass D_N^*, defined by

$$D_N^* = \frac{g_N}{f}. \tag{A11}$$

Use of (A7) in (A11) results in the simple relationship:

$$D_N^* = D_o + (1 - D_o)(D_1 + \psi_N), \quad 2 \leqslant N \leqslant \infty. \tag{A12}$$

Thus, convergence defined in the equivalent sense to (A1), namely,

$$\lim_{N\to\infty} g_N = f \tag{A13}$$

demands that D_N^*, as defined by (A12), approach unity in light of criterion (A9).

The nature of the convergence properties of the Barnes (1973) objective analysis scheme can be understood from an analysis of (A9), (A10) and (A12). It can be shown analytically that (A10) is a convergent power series, and numerically that it converges to the value given in (A9). Applying the ratio test for convergence to (A10), we have

$$\frac{D_{N+1}\prod_{j=2}^{N+1}(1 - D_{j-1})}{D_N\prod_{j=2}^{N}(1 - D_{j-1})} = \frac{D_{N+1}}{D_N}(1 - D_N) \equiv L. \tag{A14}$$

The series (A10) is absolutely convergent only if $L < 1$. Substitution of (A3) into (A14) results in

$$L = D_o^{[\gamma^{N+1}-\gamma^N]}(1 - D_o^{\gamma^N}). \qquad \text{(A15)}$$

Recalling that D_o is constant for any given choice of weight factor κ_o and has a value $0 \leq D_o \leq 1$, then L must be a constant, as required for convergence. In the limiting case as $N \to \infty$, both $\gamma^{N+1} \to 0$ and $\gamma^N \to 0$ for the range $0 < \gamma < 1$, so that $L \to 0$. Thus, there is absolute convergence in the limiting sense as $N \to \infty$.

The results of computing $D_N^*(D_o, \gamma, N)$ (Fig. A1) indicate that it converges rapidly to unity, as required. Barnes (1973) noted that the fastest restoration of small wavelength amplitude suppressed in the first pass through the data is obtained with the smallest values of γ. For a choice of $\gamma = 0.20$ and $D_o = 0.0064$, the value of D_N^* approaches 1.0 to within ten decimal places by the $N = 6$ iteration. The same degree of convergence is reached by $N = 9$ when $\gamma = 0.45$. Convergence is obtained relatively quickly even for $\gamma = 0.8$ and is attainable in a finite time as long as $\gamma < 1$. Thus, the Barnes (1973) objective analysis scheme converges to the value specified in (A9) when $0 < \gamma < 1$. It is noted that this scheme forces the interpolated fields to converge much more rapidly to the observed fields than does the Barnes (1964) scheme, as can be easily seen by comparing (A12) to equation (20) of that paper.

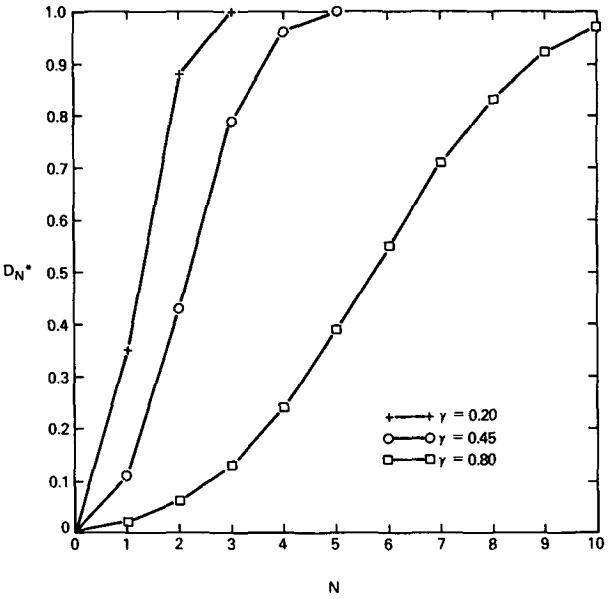

FIG. A1. Nature of Barnes analysis convergence properties.

2. Effect of multiple passes upon filter fidelity

Having thus verified that convergence is attainable, we consider whether making more than two passes through the data can effect a significant enhancement of the small, but resolvable, waves. For most purposes, it is desirable to suppress the response to a wave for which scale does not exceed twice the average minimum data spacing ($\lambda < 2\Delta n$). Considering the Gaussian nature to the response function, we note that then the final response at this minimum resolvable scale should be limited by $D_N^*(\lambda = 2\Delta n) \leq e^{-1}$. Under this constraint, high frequency noise generated by random errors and energy aliased from shorter wavelengths to larger wavelengths will be effectively filtered from the analysis. The aliased energy can result from both the data discretization process and sampling of the atmosphere when it exhibits such subgrid-scale events as thunderstorms.

Thus, the question can be rephrased as, for a given fixed weight parameter κ_o: *Can the steepness of the filter response curve at wavelengths larger than $2\Delta n$ be appreciably increased (filter fidelity enhanced) by making more than two passes, under the constraint that the final response at $\lambda = 2\Delta n$ does not exceed e^{-1}?* A comparison was made between the response curves generated by a two-pass, small γ filter (high fidelity) and those generated by multiple pass, larger γ filters.

The results of the comparison (Fig. A2) were obtained by employing the following procedure. First, the $2\Delta n$ wavelength was defined in terms of known quantities. Since the weight parameter κ_o must be held constant for the purpose of the comparison, and under this condition a singular relationship exists between any wavelength λ and the first pass response at that wavelength $D_o(\lambda)$, then a useful definition according to (2) is:

$$2\Delta n = \pi\left(\frac{-\kappa_o}{\ln D_o(2\Delta n)}\right)^{1/2}. \qquad \text{(A16)}$$

Since κ_o is constant here, one can form the ratio

$$\frac{\lambda}{2\Delta n} = \left(\frac{\ln D_o(2\Delta n)}{\ln D_o(\lambda)}\right)^{1/2}. \qquad \text{(A17)}$$

Thus, the effectiveness of making additional passes at larger γ is examined as a function of multiples of the $2\Delta n$ wavelength. Each curve in Fig. A2 is the result of the search for that value of γ which gives $D_N^*(\lambda = 2\Delta n) = e^{-1}(N > 1)$; D_N^* is then found at other wavelengths other than $\lambda = 2\Delta n$ by the following formula derived from (A17):

$$D_o(\lambda) = [D_o(2\Delta n)]^{(2\Delta n/\lambda)^2}, \qquad \text{(A18)}$$

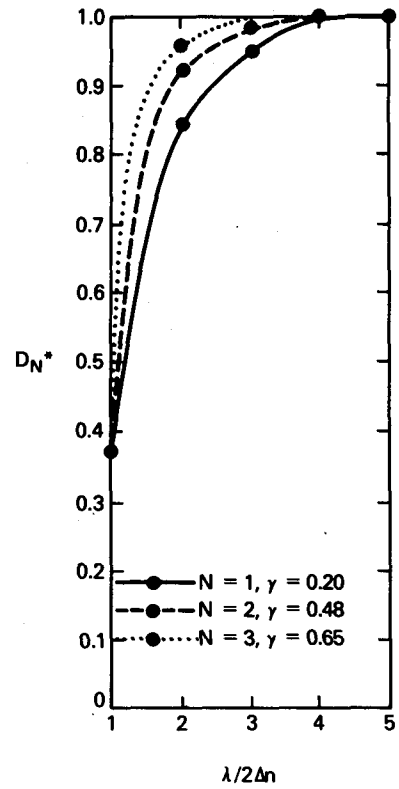

FIG. A2. Effective enhancement of filter response D_N^* produced by making multiple passes, as function of resolvable wavelengths $\lambda > 2\Delta n$.

for integral values of $(\lambda/2\Delta n)$, inserting the result in (A12) for the chosen γ value, and plotting D_N^* against multiples of the $2\Delta n$ wave according to (A17). The selected value of $D_o(2\Delta n) = 0.0064$ used in (A18) is that one which gives a second pass response of $D_1^*(2\Delta n) = 0.37 = e^{-1}$ when $\gamma = 0.2$ (see Fig. A1). The value of $\gamma = 0.2$ is chosen to represent the two-pass, small γ case.

The results in Fig. A2 show that when $N = 1$, 2, and 3 iterations through the data are made, the responses are 0.84, 0.92 and 0.96, respectively, at twice the minimum resolvable scale. Differences between these responses are no more than 12% and decrease at larger wavelengths. These differences are further attenuated when an even smaller γ value case is chosen as the basis for comparison with multiple pass filters. Thus, one correction pass using a small γ value provides for a highly acceptable degree of filter fidelity. Therefore, if one wishes to make the final objective analysis fit the data as exactly as possible, the same result can be obtained by making a greater number of interpolation passes (which is computationally wasteful and can cause greater ballooning effects in data-sparse areas), or by using a small γ value to reduce the correction pass influence radius.

REFERENCES

Barnes, S. L., 1964: A technique for maximizing details in numerical weather map analysis. *J. Appl. Meteor.*, **3**, 396–409.

——, 1973: Mesoscale objective analysis using weighted time-series observations. NOAA Tech. Memo. ERL NSSL-62, National Severe Storms Laboratory, Norman, OK 73069, 60 pp. [NTIS COM-73-10781].

Billingsley, J. B., 1976: Interactive image processing for meteorological applications at NASA/Goddard Space Flight Center. *Preprints Seventh Conf. Aerospace and Aeronautical Meteorology and Symposium on Remote Sensing from Satellites,* Melbourne, Amer. Meteor. Soc., 268–275.

Cahir, J. J., J. M. Norman and D. A. Lowry, 1981: Use of a real-time computer graphics system in analysis and forecasting. *Mon. Wea. Rev.*, **109**, 485–500.

Chesters, D., L. W. Uccellini and A. Mostek, 1982: VISSR Atmospheric Sounder (VAS) simulation experiment for a severe storm environment. *Mon. Wea. Rev.*, **110**, 198–216.

Cressman, G. P., 1959: An operational objective analysis system. *Mon. Wea. Rev.*, **87**, 367–374.

Doswell, C. A., 1977: Obtaining meteorologically significant surface divergence fields through the filtering property of objective analysis. *Mon. Wea. Rev.*, **105**, 885–892.

Fuelberg, H. E., 1974: Reduction and error analysis of the AVE II pilot experiment data. NASA Contractor Rep. CR-120496. Marshall Space Flight Center, Huntsville, AL, 140 pp.

Hasler, A. E., W. E. Shenk and W. C. Skillman, 1977: Wind estimates from cloud motion: Results from Phases I, II, and III of an *in situ* aircraft verification experiment. *J. Appl. Meteor.*, **16**, 812–815.

Hayden, C. M., 1973: Experiments in four-dimensional assimilation of Nimbus-4 SIRS data. *J. Appl. Meteor.*, **12**, 425–436.

Heymsfield, G. M., K. K. Ghosh and L. C. Chen, 1983: An interactive system for compositing digital radar and satellite data. *J. Climate Appl. Meteor.*, **22**, 705–713.

Horn, L. H., R. H. Petersen and T. M. Whittaker, 1976: Intercomparisons of data derived from Nimbus-5 temperature profiles, rawinsonde observations and initialized LFM model fields. *Mon. Wea. Rev.*, **104**, 1362–1371.

Inman, R. L., 1970: Papers on operational analysis schemes at the National Severe Storms Forecast Center. NOAA Tech. Memo. ERL NSSL-51, National Severe Storms Laboratory, Norman, OK 73069, 91 pp. [NTIS COM-71-00136].

Koch, S. E., M. desJardins and P. J. Kocin, 1981: The GEMPAK Barnes objective analysis scheme. NASA Tech. Memo. 83851, NASA/GLAS, Greenbelt, MD 20771, 56 pp. [NTIS-N8221921].

——, and J. McCarthy, 1982: The evolution of an Oklahoma dryline. Part II: Boundary-layer forcing of mesoconvective systems. *Mon. Wea. Rev.*, **39**, 237–257.

Maddox, R. A., 1980: An objective technique for separating macroscale and mesoscale features in meteorological data. *Mon. Wea. Rev.*, **108**, 1108–1121.

——, and T. H. Vonder Haar, 1979: Covariance analyses of satellite-derived mesoscale wind fields. *J. Appl. Meteor.*, **18**, 1327–1334.

Negri, A. J., and T. H. Vonder Haar, 1980: Moisture convergence using satellite-derived wind fields: A severe local storm case study. *Mon. Wea. Rev.*, **108**, 1170–1182.

Peslen, C. A., 1980: Short-interval *SMS* wind vector determinations for a severe local storm area. *Mon. Wea. Rev.*, **108**, 1407–1418.

——, S. E. Koch and L. W. Uccellini, 1982: A study of the height specification problem for satellite-derived wind vectors within a severe storm environment. *Preprints 12th Conf. Severe Local Storms,* San Antonio, Amer. Meteor. Soc., 489–492.

Petersen, R. A., L. W. Uccellini, D. Chesters, A. Mostek and D.

Keyser, 1982: The use of VAS satellite data in weather analysis, prediction, and diagnosis. *Preprints Ninth Conf. Weather Forecasting and Analysis,* Seattle, Amer. Meteor. Soc., 219–226.

Peterson, D. P., and D. Middleton, 1963: On representative observations. *Tellus,* **15,** 387–405.

Reynolds, D. W., 1983: Prototype workstation for mesoscale forecasting. *Bull. Amer. Meteor. Soc.,* **64,** 264–273.

Smith, E. A., 1975: MCIDAS system. *IEEE Trans. Geosci. Electron.,* **GE12,** 123–136.

——, T. A. Brubaker and T. H. Vonder Haar, 1978: All digital video imaging system for atmospheric research (ADVISAR). Atmos. Sci. Rep., Colorado State University, 6 pp.

Smith, W. L., H. B. Howell and H. M. Woolf, 1979: The use of interferometric radiance measurements for sounding the atmosphere. *J. Atmos. Sci.,* **36,** 566–575.

Stephens, J. J., and J. M. Stitt, 1970: Optimum influence radii for interpolation with the method of successive corrections. *Mon. Wea. Rev.,* **98,** 680–687.

Tracton, M. S., A. J. Desmarais, R. J. Van Haaren and R. D. McPherson, 1980: The impact of satellite soundings on the National Meteorological Center's Analysis and Forecast System—The Data Systems Test results. *Mon. Wea. Rev.,* **108,** 543–586.

Uccellini, L. W., and P. J. Kocin, 1981: Mesoscale aspects of jet streak coupling and implications for the short term forecasting of severe convective storms. IAMAP *Assembly Nowcasting Symposium,* Hamburg, FRG, ESA SP-165, European Space Agency, 75738 Paris 15, France, 375–380.

Wilson, T. A., and D. D. Houghton, 1979: Mesoscale wind fields for a severe storm situation determined from SMS cloud observations. *Mon. Wea. Rev.,* **107,** 1198–1209.